Molecular Transport of Alkanes Through Thermoplastic Miscible Blends of Ethylene–Propylene Random Copolymer and Isotactic Polypropylene

TEJRAJ M. AMINABHAVI* and HEMANT T. S. PHAYDE

Department of Chemistry, Karnatak University, Dharwad 580 003, India

SYNOPSIS

A new experimental protocol based on the measurements of sorption (S), desorption (D), resorption (RS), and redesorption (RD) has been used to study the molecular transport of aliphatic alkanes through the miscible blends of an ethylene–propylene random copolymer and an isotactic polypropylene over the temperature interval 25–70°C. Diffusion and activation parameters are evaluated and their dependencies on solvent size, shape, and nature are discussed. Estimated values of the molar mass between chain entanglements, kinetic rate constants, and overshoot index parameters have been influenced by the polymer–solvent interactions. The sorption–diffusion mechanism is found to be of anomalous type.

INTRODUCTION

Molecular transport of organic solvents into polymeric materials has been the subject of both technological and fundamental interest in a variety of applications such as controlled drug release,[1,2] microelectronics,[3] polymer processing industries,[4] food packaging,[5,6] and separation science.[7–9] Research in this area has been quite active in the past decades and a variety of polymer–solvent systems have been investigated with reference to their transport-based interactions. However, the molecular transport problem is rather complex because by changing the polymer–penetrant pair or simply the operating conditions several different types of transport behaviors could be observed.[10] On the basis of integral sorption (or desorption) data, solvent transport into a rubbery polymer is found to follow the Fickian behavior with a diffusion coefficient that is dependent on the penetrant concentration. In contrast to this behavior, mass transport deviates from Fickian behavior in cases where the solvent has a limited solubility in the polymer. This exhibits a strong concentration dependence of the diffusivity.

Miscible blends of an ethylene–propylene random copolymer and an isotactic polypropylene, also known as Santoprene, belongs to a family of advanced elastomers that successfully combines the performance characteristics of vulcanized rubber such as heat resistance and low compression set with the processing ease of thermoplastics. In view of its dual advantages of low-cost thermoplastic processing and vulcanized rubber performance, it finds applications as pump-related gaskets, hose connectors, windshield spacers, air ducts, expansion joints, vibration isolators, flexible cords, submersible cable, pump seals, etc. However, acceptability of Santoprene for any specific application depends ultimately on its solvent-transport characteristics and, therefore, the end-use performance testing is important before Santoprene seeks commercial or engineering applications. The understanding of Santoprene interactions with solvents is therefore critical to the prediction of its behavior in applications where it is exposed to solvent.

Solvent sorption and diffusion are the limiting factors of polymer end-use applications because these processes might change the mechanical properties and sometimes cause destruction in polymer structures. An investigation of the causes of such phenomena requires a thorough knowledge of the solvent-transport characteristics. Diffusion coefficients (D) and equilibrium solvent sorption (M_∞) are the fundamental parameters measured during

* To whom correspondence should be addressed.

Journal of Applied Polymer Science, Vol. 55, 1335–1352 (1995)
 CCC 0021-8995/95/091335-18

solvent sorption. Several studies have indicated that the weight gain curves for polymers immersed in different solvents show a decrease after reaching a maximum.[11-14] This phenomenon was attributed to a leaching-out effect. Therefore, it is important to know whether a polymer undergoing weight loss is losing residuals or whether the polymer morphology is altered. In some polymeric systems, the presence of solvents produced an overshoot effect followed by a steady decline to an equilibrium position.[15-22] Such effects are the result of polymer rapid relaxation processes during solvent migration. The cause of the overshoot effect and its relation to structural characteristics of the polymer were addressed earlier.[15-22]

The purpose of the present study was to investigate the Santoprene–solvent interactions as a function of temperature, solvent size, polymer morphology, solvent sorption, and diffusion characteristics. During this work, a technique was used to assess the polymer weight loss and, hence, to determine the sorption parameters. After sorption, polymer samples were desorbed to measure the amount of sorbed solvent and removal of any residuals. The desorbed samples were again exposed to solvent for resorption followed by redesorption. Therefore, it appears that sorption (S)–desorption (D)–resorption (RS)–redesorption (RD), designated as S–D–RS–RD testing, is an effective analytical probe for studying polymer–solvent interactions and to obtain the true equilibrium values and diffusion coefficients.

Previous articles from our laboratory[23-25] were concerned with molecular transport (sorption, permeation, and diffusion) studies of polymer membranes in the presence of *n*-alkanes as penetrants. As a further contribution, we present here the sorption, desorption, and diffusion results of Santoprene in the presence of aliphatic alkanes over the temperature interval 25–70°C. The values of the sorption coefficients were obtained from the equilibrium sorption data, whereas the diffusion coefficients were calculated from the sorption results. The temperature dependencies of sorption, diffusion, and permeation coefficients were used to estimate the activation parameters for each of these processes. The experimental results are discussed in terms of the interactions of Santoprene chain segments with chemically and structurally different alkanes.

EXPERIMENTAL

Reagents and Materials

Santoprene (sample designation #101-80) sheets of nearly uniform initial thicknesses ranging from 0.147 to 0.156 cm with dimensions of 26 × 26 cm were obtained from Advanced Elastomer Systems, St. Louis, Missouri. Circular disc-shaped samples (diameter = 1.96–1.98 cm) were cut from large Santoprene sheets by using a sharp-edged carbon-tipped steel die. The Santoprene samples were dried in vacuum desiccators over anhydrous calcium chloride at room temperature for at least 24 h before use. Some typical fluid resistance properties of Santoprene are given in Table I.

The reagent-grade solvents used as penetrants are *n*-pentane (BDH, England), *n*-hexane and *n*-heptane (both S.D. Fine Chem. Ltd., Bombay, India), *n*-octane (Riedel, Germany), *n*-nonane, *n*-decane, *n*-dodecane, *n*-tetradecane, and *n*-hexadecane (all from S.D. Fine Chem. Ltd.), 2,2,4-trimethylpentane (BDH), cyclohexane (Ranbaxy Labs. Ltd., Punjab, India), and 1,2,3,4-tetrahydronaphthalene (Riedel). Of these, 2,2,4-trimethylpentane, *n*-dodecane, and 1,2,3,4-tetrahydronaphthalene were double-distilled before use, whereas other solvents were used as supplied. Their measured density and refractive index values at 25°C agreed well with the literature values[26]; however, these data are not tabulated, but some relevant solvent properties are given in Table II.

Sorption (S)–Desorption (D)–Resorption (RS)–Redesorption (RD) Experiments

Dried Santoprene samples weighing initially (W_0) ≈ 0.4455 g were placed in screw-tight test bottles containing 15–20 mL of the solvents. The samples were removed periodically, and the surface-adhered liquid drops were removed by carefully pressing the samples in between filter paper wraps and weighed

Table I Typical Fluid Resistance Properties of Santoprene Tested for 166 h

Fluid	Test Temp (°C)	Volume Swelling (%)
Water	100	3
15% NaCl	23	0
50% NaOH	23	0
98% H_2SO_4	23	3
ASTM #1 oil	100	17
ASTM #2 oil	100	34
ASTM #3 oil	100	50
Brake fluid	100	−14
Automatic transmission fluid	125	47

Table II Some Physical Properties of Solvents Used as Penetrants at 25°C

Alkane	bp (°C)	η (mPa-s)	ε	V (cm^3/mol)	$R \times 10^{3}$ [a]	δ (cal cm^{-3})$^{1/2}$
n-Pentane	36	0.23[b]	1.84[b]	115.2	—	7.10
n-Hexane	69	0.29	1.88	131.6	1.35	7.27
n-Heptane	98	0.40	1.93	147.5	1.54	7.43
n-Octane	126	0.52	1.95	163.5	1.72	7.57
n-Nonane	151	0.67	1.97	179.7	1.91	7.65
n-Decane	174	0.86	1.99	195.9	2.09	7.72
n-Dodecane	216	1.38	2.00	228.6	2.48	7.84
n-Tetradecane	254	2.04	2.04	260.1	2.85	7.96
n-Hexadecane	287	3.01	2.09	292.8	3.22	8.01
2,2,4-Trimethylpentane	99	0.47	1.94	166.1	1.70	6.85
Cyclohexane	81	0.90	2.02[b]	108.8	—	8.20
1,2,3,4-Tetrahydronaphthalene	208	2.00	2.77	136.8	1.55	9.50

[a] ($[ms^{-1}]^{1/3}$ m^3 mol^{-1}).
[b] At 20°C.

(W_t) on a digital Mettler balance, Model AE 240 (Switzerland), to an accuracy of ±0.01 mg. Samples reached equilibrium saturation within 24 h, which did not change significantly over a further period of 1 or 2 days. The percent weight gain (wt %) during solvent sorption was calculated as

$$Wt\ gain\ \%\ (t) = \left(\frac{W_t - W_0}{W_0}\right) \times 100 \qquad (1)$$

After sorption experiments, the sorbed samples were placed in vacuum for desorption measurements. The decrease in mass was monitored periodically. The total weight loss after desorption was calculated as

$$Wt\ loss\ \% = \left(\frac{W_0 - W_d}{W_0}\right) \times 100 \qquad (2)$$

where W_d is mass of the polymer after desorption.

The resorption testing was carried out in the same manner as were the sorption tests. Data on each sample, including mass and time measurements, were recorded and stored in a computer for subsequent analysis. If Santoprene does not show any mass loss during sorption and desorption, the initial mass of Santoprene and mass after desorption will be the same. However, in the present investigation, mass loss in Santoprene occurred during sorption. If after sorption and desorption runs, Santoprene released all its species contributing to weight loss; the desorption equilibrium solvent content and resorption equilibrium solvent content should be the same. The resorbed samples were placed once again in vacuum for a second desorption. Any difference between the mass loss after redesorption indicates the continued mass loss during resorption. This comparison is another way of determining the extent of continuous loss, if any, during the S–D–RS–RD testing. The observed total losses in the S–D–RS–RD experiments are listed in Table III. The mol % weight changes in resorption experiments are generally higher than those observed in sorption experiments, indicating higher sorption values. However, for desorption and redesorption experiments, the mol % mass changes remain almost the same for all liquids. The total percent mass losses in sorption–desorption cycles are higher than those observed in resorption–redesorption cycles and these vary in the range 34–36 wt %, suggesting leaching out of the additives from the Santoprene matrix.

RESULTS AND DISCUSSION

Sorption Behavior

Continuing our earlier approaches,[23–25] the dynamic penetrant sorption results were analyzed using the empirical equation[15,16]

$$\frac{M_t}{M_\infty} = Kt^n \qquad (3)$$

where M_t is the mass of solvent sorbed at time t; M_∞, the mass of solvent sorbed at equilibrium; and K, a system parameter that depends on the struc-

Table III Mol Percent Weight Change and Total Weight Loss During Sorption (S)–Desorption (D)–Resorption (RS)–Redesorption (RD) Experiments at 25°C

	Mol % Wt Change				Total % Weight Loss After	
Alkane	S	D	RS	RD	S–D Cycle	RS–RD Cycle
n-Pentane	0.195	0.621	1.080	0.636	36.2	2.75
n-Hexane	0.280	0.572	1.051	0.553	36.1	0.56
n-Heptane	0.293	0.505	0.973	0.502	36.0	1.92
n-Octane	0.334	0.473	1.013	0.470	36.2	1.05
n-Nonane	0.256	0.402	0.803	0.406	35.6	1.78
n-Decane	0.234	0.367	0.751	0.365	36.3	0.46
n-Dodecane	0.188	[a]	—	—	34.3	—
n-Tetradecane	0.165	[a]	—	—	35.1	—
n-Hexadecane	0.149	[a]	—	—	[a]	—
2,2,4-Trimethylpentane	0.192	0.418	0.761	0.414	36.2	1.57
Cyclohexane	0.772	0.720	1.931	0.752	34.9	3.63
1,2,3,4-Tetrahydronaphthalene	0.469	0.466	1.085	0.419	35.9	[b]

[a] Data not obtained due to their high boiling points.
[b] Data not obtained.

tural characteristics of the Santoprene and on Santoprene–penetrant interactions. The exponent value of n suggests the type of transport mechanism. In desorption, M_t and M_∞ represent, respectively, the mass loss of the drying samples at time t and the completely dried samples. Equation (3) is applicable for a preliminary analysis of sorption data, i.e., up to 55% of equilibrium sorption and it does not provide evidence for such details as inflections or solvent loss with time. The estimated values of n (along with the error estimates) and K for sorption and resorption runs are compiled in Table IV.

Table IV Estimated Values of n and K (g/g min^n) from Eq. (3) for Santoprene + Alkanes Along With the Error Values (σ) for n

	$n \pm \sigma$		K (× 10)	
	S	RS	S	RS
Alkane	25–70°C	25°C	25–70°C	25°C
n-Pentane	0.62 ± 0.007	0.63 ± 0.036	2.80	0.81
n-Hexane	0.55–0.59 ± 0.008[a]	0.62 ± 0.033	1.67–2.31[a]	0.65
n-Heptane	0.58–0.74 ± 0.013	0.63 ± 0.033	1.58–2.05	0.54
n-Octane	0.57–0.62 ± 0.010	0.63 ± 0.023	1.17–1.95	0.46
n-Nonane	0.57–0.58 ± 0.009	0.61 ± 0.025	1.17–1.92	0.42
n-Decane	0.57–0.58 ± 0.005	0.60 ± 0.020	0.99–1.43	0.39
n-Dodecane	0.54–0.57 ± 0.004	[b]	0.82–1.31	[b]
n-Tetradecane	0.55–0.57 ± 0.005	[b]	0.65–1.07	[b]
n-Hexadecane	0.54–0.56 ± 0.004	[b]	0.52–0.98	[b]
2,2,4-Trimethylpentane	0.55–0.58 ± 0.010	0.58 ± 0.022	1.15–1.63	0.37
Cyclohexane	0.59–0.66 ± 0.008	0.62 ± 0.023	0.73–1.04	0.38
1,2,3,4-Tetrahydronaphthalene	0.52–0.61 ± 0.009	0.58 ± 0.019	0.66–1.05	0.26

[a] 25–55°C.
[b] Data not obtained due to their high boiling points.

In the majority of systems, the values of n for sorption runs vary between 0.52 and 0.74 over the temperature interval 25–70°C, suggesting the transport to be of an anomalous type.[27-30] In the case of resorption runs at 25°C, the values of n vary from 0.58 to 0.63. The values of K increase with increasing temperature and also show a dependence on solvent size. Thus, K values decrease from n-pentane to n-hexadecane, suggesting decreased polymer–solvent interactions. The values of K for cyclohexane are higher than for 1,2,3,4-tetrahydronaphthalene. The dependence of K on the number of carbon atoms of n-alkanes in the investigated temperature range is shown in Figure 1. For resorption runs, the values of K are nearly two to three times smaller when compared to sorption runs, indicating somewhat mild interactions.

The sorption results are presented using the normalized parameter, $t^{1/2}/h$, to avoid any differences in the thicknesses of Santoprene sheets. Thus, the reduced plots of S–D–RS–RD runs for lower n-alkanes, i.e., C_5 to C_{10}, including 2,2,4-trimethylpentane, i.e., C_8 at 25°C, are presented in Figure 2. Initially, the uptake values showed an overshoot effect for sorption runs. The observed sharp maxima are then declined back to the true equilibrium values. Such overshooting has been analyzed as a function of polymer cross-link density, geometrical characteristics of the polymer, and increased mobility of the polymer chains.[15,16] Another plausible reason for the observed overshoot effect may be attributed to the presence of a thin layer formed during polymerization, which is morphologically different from the bulk of the polymer.[17] Several other studies addressed different aspects of the overshoot phenomenon as polymers absorb solvents.[18-22] However,

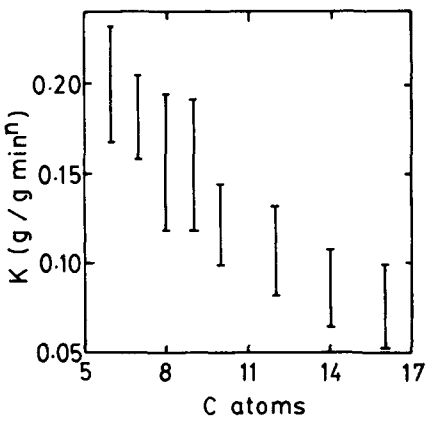

Figure 1 Dependence of parameter K of eq. (3) on number of carbon atoms of n-alkanes: Vertical bars indicate the temperature interval of 25–70°C.

overshoot was not observed for desorption, resorption, and redesorption runs as shown in Figure 2.

The observed overshoot effect has been analyzed from a calculation of the percent overshoot index, OI, as[16]

$$OI = \frac{M_{max} - M_\infty}{M_\infty} \times 100 \qquad (4)$$

where M_{max} represents the maximum value of the penetrant uptake. These values at different temperatures are given in Table V. The values of OI do not exhibit any relationship with the size of alkane molecules. The value of OI at 25°C for n-pentane is the highest, i.e., 91.5, and these values decrease from n-hexane to n-octane. The values of OI for n-nonane are higher than those of n-octane at all temperatures. However, no systematic dependence of OI on temperature is observed. The OI for 2,2,4-trimethylpentane is higher than for n-octane, and for 2,2,4-trimethylpentane, OI decreases with increase in temperature. The dependence of OI on the number of carbon atoms of n-alkanes is displayed in Figure 3. At higher temperatures. The OI values decrease with increasing penetrant size. The observed lower values of OI for the bigger alkanes is attributed to a slow relaxation of polymer-chain segments.

In a sorption–desorption cycle, the available free volume of the Santoprene matrix might increase and, hence, the subsequent sorption process is different from the original. These effects have been successfully described by the polymer network relaxation, the times required for the molecular rearrangements of the chains, and that of solvent diffusion into the network polymer.[31] However, segmental mobility of Santoprene might also increase due to solvent sorption and this depends on the interaction of solvent molecules with Santoprene chain segments in addition to the availability of the fractional free volume.

The resorption curves at 25°C for 2,2,4-trimethylpentane and n-decane are almost identical (Fig. 2). Similarly, for n-pentane and n-hexane, the sorption curves are somewhat identical. On the other hand, the resorption values of n-octane are higher than those of n-pentane. The sorption and resorption curves for higher alkanes are not presented graphically to avoid overcrowding of plots. However, noticeable overshoot effects can be seen with cyclohexane, 1,2,3,4-tetrahydronaphthalene, and n-dodecane; these effects tend to diminish slowly in case of n-tetradecane and n-hexadecane. Also, the equilibrium sorption values are considerably lower for

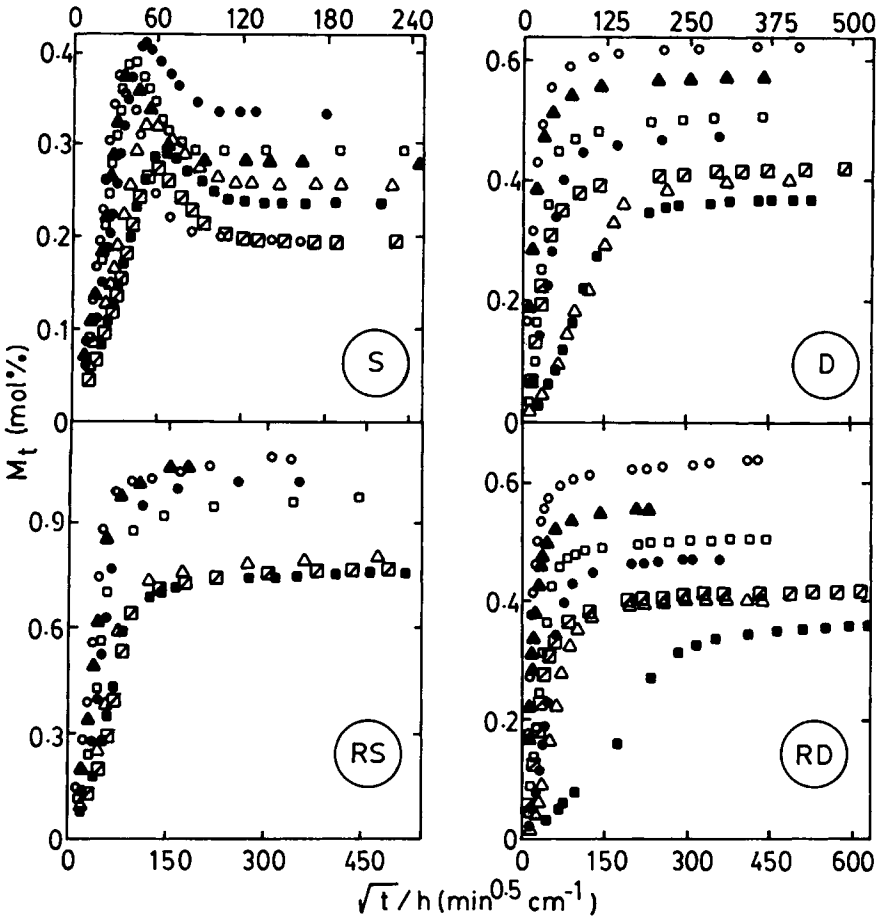

Figure 2 Reduced plots of mol % sorption, desorption, resorption, and redesorption at 25°C for (○) *n*-pentane, (▲) *n*-hexane, (□) *n*-heptane, (●) *n*-octane, (△) *n*-nonane, (■) *n*-decane, and (▨) 2,2,4-trimethylpentane.

the long-chain *n*-hexadecane when compared to the cyclic penetrants, viz., cyclohexane and 1,2,3,4-tetrahydronaphthalene. It is, however, striking to observe a systematic increase in mol % desorption from C_5 to C_8. The desorption curves for 2,2,4-trimethylpentane, *n*-nonane, and *n*-decane are slightly sigmoidal, suggesting their higher interactions with Santoprene segments. The desorption runs for C_{12}, C_{14}, and C_{16} are not performed due to the difficulties in completely drying the polymer samples, as these solvents possess high boiling points (Table II).

The redesorption curves follow almost identical patterns like those observed for desorption processes. However, the equilibrium uptake values and the time required to reach the true equilibrium desorption are higher in redesorption runs compared to desorption. A striking difference is seen in the case of *n*-decane, which shows a more sigmoidal tendency for the redesorption process than for desorption. Also, the equilibrium desorption values for *n*-nonane and 2,2,4-trimethylpentane are almost identical. However, during the second desorption cycle, a slight departure from Fickian behavior is observed in the case of *n*-decane. It may be noted that the transport behavior of 2,2,4-trimethylpentane is very different in all the S–D–RS–RD experiments, i.e., it exhibits a lower mol % value than do all the other penetrants. However, in desorption runs, its value is higher than that of *n*-decane.

The results presented in Figure 4 serve as a typical example of the effect of temperature on the observed sorption behavior of *n*-heptane, *n*-dodecane, *n*-hexadecane, and 1,2,3,4-tetrahydronaphthalene. The overshoot effects are persistent even at higher temperatures, but the effect is not systematic. For 1,2,3,4-tetrahydronaphthalene, the temperature-dependent sorption curves increase systematically with temperature. Equilibrium uptake values for *n*-heptane and *n*-hexadecane lie within a narrow range, whereas those for *n*-dodecane lie over a wide range.

Table V Percent Overshoot Index, *OI*, Interaction Parameter, χ, and Molar Mass, $\bar{M}_C$, Between Chain Entanglements

Alkane	*OI*				χ	$\bar{M}_C$
	25°C	40°C	55°C	70°C		
n-Pentane	91.5	[a]	[a]	[a]	0.383	92
n-Hexane	37.8	34.3	43.1	[a]	0.360	169
n-Heptane	33.0	36.0	36.0	39.2	0.345	223
n-Octane	22.6	22.2	23.0	28.2	0.340	328
n-Nonane	24.9	26.5	26.7	29.0	0.342	292
n-Decane	23.7	25.4	23.2	24.7	0.347	320
n-Dodecane	26.3	24.8	27.1	26.8	0.368	357
n-Tetradecane	20.4	21.6	20.8	20.3	0.407	433
n-Hexadecane	14.1	18.4	16.4	19.6	0.436	521
2,2,4-Trimethylpentane	40.7	39.2	38.3	37.6	0.485	217
Cyclohexane	4.9	10.4	7.8	7.2	0.413	461
1,2,3,4-Tetrahydronaphthalene	7.7	8.3	6.4	2.1	1.201	[b]

[a] Data not obtained due to their low boiling points.
[b] Negative value observed.

A plausible explanation for this effect is that at high penetrant concentration, i.e., during the later stages of sorption, the distribution of solvent molecules into the dense region of the polymer becomes significant. Also, at this stage, a significant change in the molecular structure of the network might occur.

In desorption, however, a major portion of the polymer void region is collapsed, producing a mismatch between the diffusion time and Santoprene chain rearrangement. However, in the resorption process, large-scale molecular rearrangements may not take place and diffusion may be considered merely a hole-filling process with a somewhat milder concentration dependency of diffusivity (Fig. 2). The equilibrium uptake in resorption is higher than that observed in sorption, probably due to the extra free volume formed during resorption. This also might result in the differences of the nature of the curves in sorption and resorption processes.

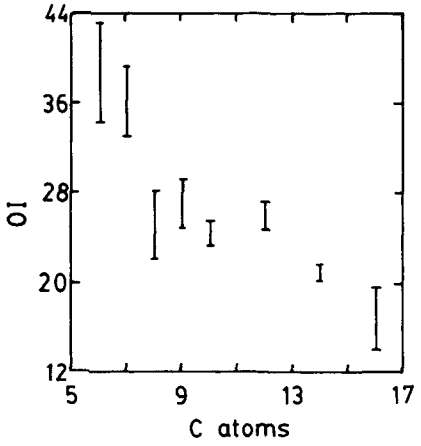

Figure 3 Dependence of overshoot index (*OI*) on number of carbon atoms of *n*-alkanes at 25°C.

The mol % sorption coefficients, *S*, obtained from the plateau regions of equilibrium sorption for sorption and resorption processes are given in Table VI. Generally, it is found that the *S* values for sorption are nearly three times smaller than those observed in resorption runs at 25°C. The *S* values for sorption runs increase from *n*-pentane to *n*-octane, but decrease from *n*-nonane to *n*-hexadecane. The values of *S* for 2,2,4-trimethylpentane are much smaller than those of *n*-octane. A longer and bigger *n*-hexadecane exhibits an equilibrium sorption of 0.149 mol % when compared to a value of 0.195 mol % for *n*-pentane. The *S* values for *n*-pentane (0.195 mol %) and 2,2,4-trimethylpentane (0.192 mol %) are almost identical. The same dependency is observed for sorption runs at higher temperatures.

It is intriguing to note that the equilibrium resorption values at 25°C show a decrease with increasing size of *n*-alkanes. The dependence of maximum and equilibrium sorption values on the size of *n*-alkanes, expressed as number of carbon atoms, is given in Figure 5. It is noticed that with the exception of *n*-octane all the other *n*-alkanes exhibit a continuous decrease in *S* with increasing size of *n*-alkanes. From the sorption results of Table VI, it is observed that although 2,2,4-trimethylpentane has 8 carbon atoms its sorption is not identical to *n*-octane, but is lower. Also, the cyclic liquids, viz., cyclohexane and 1,2,3,4-tetrahydronaphthalene, exhibit higher sorption values than the linear *n*-al-

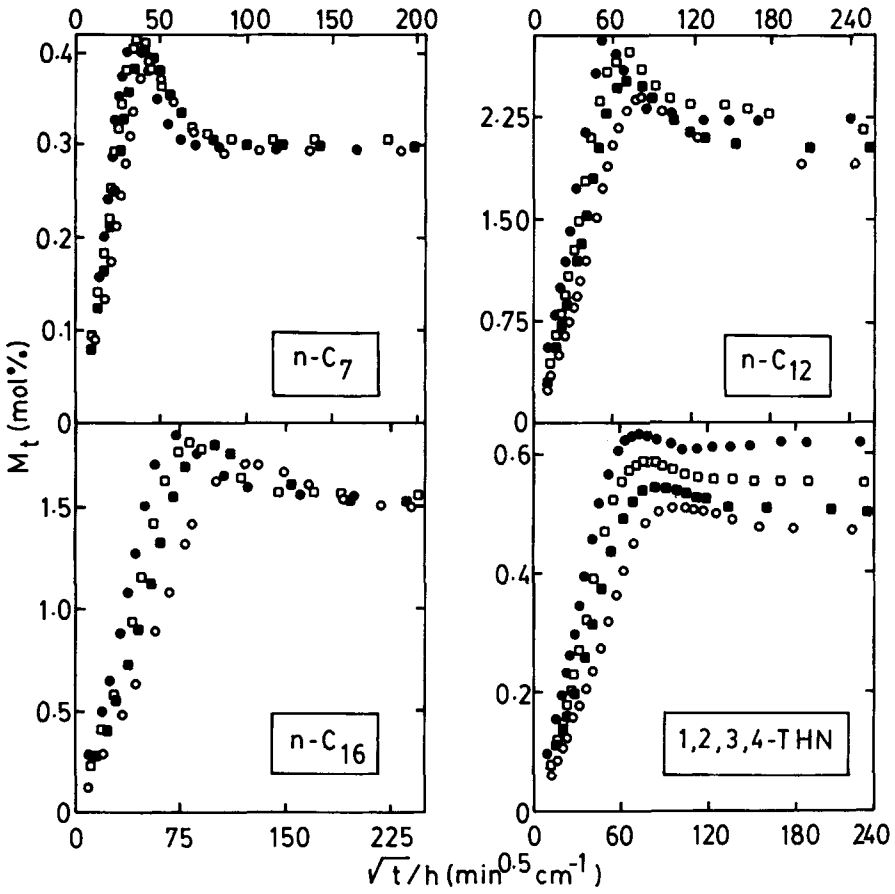

Figure 4 Effect of temperature on S–D–RS–RD curves for *n*-heptane, *n*-dodecane, *n*-hexadecane, and 1,2,3,4-tetrahydronaphthalene. Symbols: (○) 25°C; (■) 40°C; (□) 55°C; (●) 70°C.

kanes. Sorption experiments of *n*-pentane at higher temperatures and that of *n*-hexane at 70°C were not performed due to their low boiling temperatures. However, the equilibrium sorption values for *n*-hexane are slightly smaller than those for *n*-heptane at 25°C, but, at 40° and 55°C, sorption of *n*-hexane and *n*-heptane are somewhat identical. There is generally a systematic increase in equilibrium sorption with increasing temperature, with few exceptions.

Various parameters are critical in the interpretation of sorption data. These are temperature, penetrant size, shape, and solvent polarity in addition to polymer sample history. An increase in temperature should normally increase sorption. Within the investigated temperature range, the dynamic penetrant sorption data tend to increase in the temperature interval from 25 to 70°C for all liquids except *n*-heptane, *n*-octane, and *n*-hexadecane. For the latter liquids, the values of S decrease with increase in temperature from 55 to 70°C. This is indicative of the fact that at 70°C these liquids might have interacted strongly with the Santoprene chain segments, thereby leaching out some of the indigenous low molecular weight additives and thus exhibiting lower equilibrium uptake.

In service conditions of a polymer, the times to attain equilibrium and maximum sorption also play an important role. Different equilibrium times (T_∞) and maximum times (T_{max}) are observed depending on the size of the penetrant molecule. Generally, the maximum as well as equilibrium times increase steadily with the increasing size of the penetrant molecules (Fig. 6). However, both T_{max} and T_∞ plots show a systematic dependence on the chain length of *n*-alkanes.

Analysis of Sorption and Desorption Measurements—Calculation of Diffusion Coefficient

The diffusion coefficient, D, of a penetrant into the network polymer can be calculated from a solution

Table VI Sorption (S, mol %) Coefficients for Santoprene + Alkanes at Different Temperatures Obtained from Sorption and Resportion Experiments

	Temperature (°C)				
	25		40	55	70
Alkane	S	RS		S	
n-Pentane	0.195	1.080	[a]	[a]	[a]
n-Hexane	0.280	1.051	0.295	0.302	[a]
n-Heptane	0.293	0.973	0.297	0.304	0.294
n-Octane	0.334	1.013	0.353	0.360	0.299
n-Nonane	0.256	0.803	0.265	0.283	0.283
n-Decane	0.234	0.751	0.239	0.265	0.272
n-Dodecane	0.188	[b]	0.201	0.213	0.222
n-Tetradecane	0.165	[b]	0.166	0.179	0.186
n-Hexadecane	0.149	[b]	0.152	0.155	0.154
2,2,4-Trimethylpentane	0.192	0.761	0.204	0.210	0.215
Cyclohexane	0.772	1.931	0.802	0.907	0.950
1,2,3,4-Tetrahydronaphthalene	0.469	1.085	0.501	0.550	0.617

[a] Data not obtained due to their low boiling points.
[b] Data not obtained due to their high boiling points.

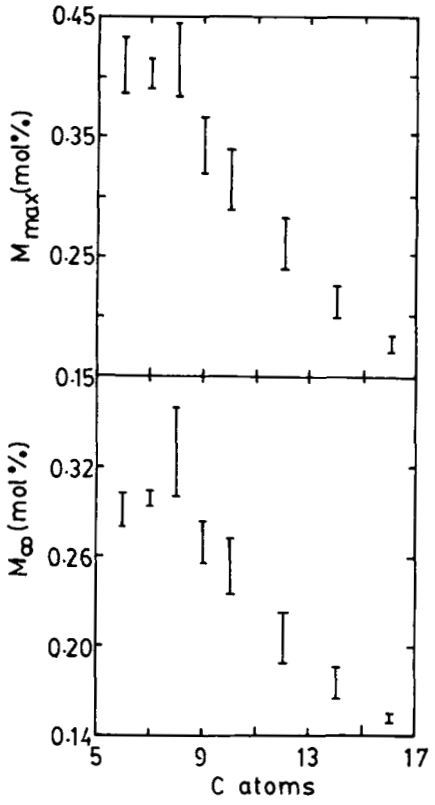

Figure 5 Dependence of maximum (M_{max}) and equilibrium (M_∞) sorption values on the number of carbon atoms of *n*-alkanes. Vertical bars indicate the temperature interval of 25–70°C.

of the Fick's second law of diffusion.[10] For a sheet geometry of the Santoprene sample immersed in an infinite bath of the liquid, Crank[10] reported different solutions of Fick's second law depending on the initial and boundary conditions. The case of interest in this article is that of a free film of thickness h, exposed to a uniform and average concentration of a diffusant (considered as a constant) and is given as

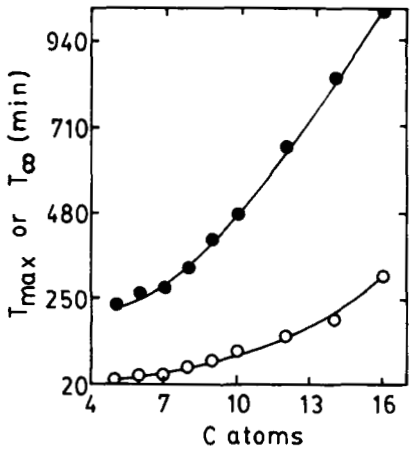

Figure 6 Dependence of (○) maximum (T_{max}) and (●) equilibrium (T_∞) times on the number of carbon atoms of *n*-alkanes at 25°C.

$$M_t = 2M_\infty\left(\frac{Dt}{h^2}\right)^{1/2} \times \left\{\frac{1}{\pi^{1/2}} + 2\sum_{n=0}^{\infty}(-1)^n i\ \text{erf}\ C\left[\frac{nh}{(Dt)^{1/2}}\right]\right\} \quad (5)$$

According to eq. (5), the plot of the fractional equilibrium uptake vs. $t^{1/2}/h$ is linear at small times and, hence, D can be calculated by the iterative procedure. However, for computational purposes, the following relation is preferred:

$$\frac{M_t}{M_\infty} = 1 - \left(\frac{8}{\pi^2}\right) \times \sum_{n=0}^{\infty}\left\{\left[\frac{1}{(2n+1)^2}\right]\exp\left[\frac{-D(2n+1)^2\pi^2 t}{h^2}\right]\right\} \quad (6)$$

The results of D calculated for S–D–RS–RD runs by the iterative procedure for the first 11 points, i.e., $n = 10$, are given in Table VII. Equation (6) at longer diffusion times can be simplified to give

$$\ln(1 - M_t/M_\infty) = \ln\left(\frac{8}{\pi^2}\right) - \frac{D\pi^2 t}{h^2} \quad (7)$$

Thus, a plot of $\ln(1 - M_t/M_\infty)$ vs. t should be linear at long diffusion times and the slope is directly proportional to D. Some of our data plotted in this format are in conformity with eq. (7) (Fig. 7).

Diffusion coefficients obtained from eq. (7) are slightly (generally 3–4%) higher than those calculated from eq. (6). This is expected because of the consideration of the long-term diffusivity while calculating D from eq. (7). However, we regard the values of D calculated from eq. (6) as more reliable. The decrease in D from n-pentane to n-hexane is quite considerable when compared with n-hexane to n-hexadecane. A systematic decrease in D is observed at all temperatures for all liquids, suggesting the dependence of D on the molecular size of the penetrants. A plot of D vs. the number of carbon atoms displaying this effect is shown in Figure 8.

It is well known that the shape of the penetrant molecule has an effect on its transport characteristics.[32–34] Linear and flexible molecules like n-alkanes might diffuse quicker than will less flexible and less symmetrical molecules like 2,2,4-trimethylpentane, cyclohexane, and 1,2,3,4-tetrahydronaphthalene. In the present research, it was found that at all temperatures the values of D for 2,2,4-trimethylpentane are lower than are the expected values of a linear molecule of the same size, i.e., n-octane. This is because the pendent methyl groups in 2,2,4-trimethylpentane with its larger diameter may not locate an appropriate hole size in the polymer matrix. Such a dependence was also observed earlier,[35] wherein the side methyl groups in hydrocarbon penetrants showed lower D values than did the linear molecules. Conversely, when liquids are

Table VII Diffusion ($D \times 10^6$, cm²/s) Coefficients for Santoprene + Alkanes at Different Temperatures Obtained from Sorption and Resorption Experiments

	Temperature (°C)						
	25		40	55	70	25	
Alkane	S	RS	S			D	RD
n-Pentane	8.42	0.73	[a]	[a]	[a]	2.63	2.86
n-Hexane	3.18	0.56	4.09	5.39	[a]	2.65	2.29
n-Heptane	2.79	0.37	3.64	4.57	5.18	0.44	0.38
n-Octane	1.67	0.34	2.16	2.87	4.51	0.35	0.12
n-Nonane	1.59	0.23	2.12	2.76	3.93	0.05	0.10
n-Decane	1.18	0.20	1.65	1.96	2.56	0.03	0.01
n-Dodecane	0.81	[b]	1.09	1.39	1.87	[b]	—
n-Tetradecane	0.51	[b]	0.70	1.02	1.36	[b]	—
n-Hexadecane	0.33	[b]	0.55	0.69	1.04	[b]	—
2,2,4-Trimethylpentane	1.53	0.16	1.89	2.38	2.87	0.50	0.43
Cyclohexane	0.77	0.24	1.14	1.52	1.69	1.04	0.47
1,2,3,4-Tetrahydronaphthalene	0.53	0.09	0.73	0.79	1.07	0.01	[c]

[a] Data not obtained due to their low boiling points.
[b] Data not obtained due to their high boiling points.
[c] Results are not reliable to report.

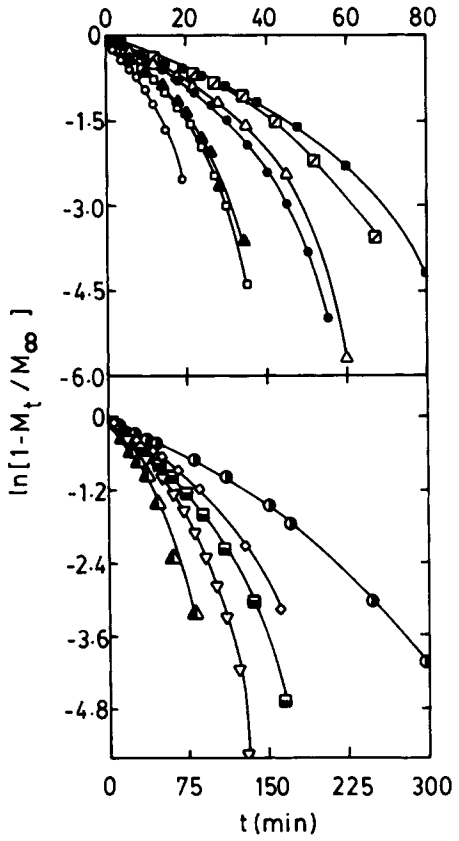

Figure 7 Long-term diffusion plots for Santoprene + alkanes at 25°C. Symbols: (▽) *n*-dodecane; (◇) *n*-tetradecane; (◑) *n*-hexadecane; (▲) cyclohexane; (■) 1,2,3,4-tetrahydronaphthalene, and remaining symbols are the same as in Figure 2.

of comparable diameter but of different lengths, the effect of the length of the molecule will also play an important role on its transport characteristics. This appears to be the case for *n*-hexadecane, for which D values are smaller than those of all other lower *n*-alkanes. Diffusion coefficients of cyclohexane are somewhat comparable to *n*-dodecane and those of 1,2,3,4-tetrahydronaphthalene are comparable to *n*-tetradecane at 25 and 40°C, in spite of their differences in molecular sizes.

The classical Fickian sorption feature is that both sorption and desorption curves should vary linearly with $t^{1/2}/h$ initially up to 55–60% equilibrium. In some cases (e.g., with *n*-pentane), the linear sorption region extends up to almost 70% of M_∞. This may be attributed to its small size. However, in general, diffusion into solid polymers depends on the availability of appropriate molecular size holes in the network in addition to the attractive forces between the penetrant molecules and the polymer. The presence of holes is determined mainly by the polymer structure and its morphology, as studied in terms of chain-entanglement densities and its dependence on solvent sorption. Santoprene, being a lightly cross-linked structure, shows a systematic dependence on chain-entanglement density, and hence, a dependence on molar mass, $\bar{M}_C$, between chain entanglements should be observed. To see this effect, efforts were made to estimate $\bar{M}_C$ values from the equilibrium swelling data using the Flory–Rehner theory[36,37] given as

$$\bar{M}_C = \frac{-\rho_P V_S[\phi_P^{1/3} - \phi_P^{1/2}]}{\ln(1 - \phi_P) + \phi_P + \chi\phi_P^2} \tag{8}$$

where V_S is the molar volume of the solvent; ρ_P, the polymer density; ϕ_P, the volume fraction of the polymer in the swollen state, and χ, the Flory–Huggins polymer–solvent interaction parameter. Volume fraction of the polymer in the swollen state has been computed by using

$$\phi_P = \left[1 + \frac{\rho_P}{\rho_S}\left(\frac{M_a}{M_b}\right) - \frac{\rho_P}{\rho_S}\right]^{-1} \tag{9}$$

where M_b and M_a are, respectively, the mass of the polymer before and after swelling; ρ_S, the solvent density; and ρ_P, the density of Santoprene.

The polymer–solvent interaction parameter, χ, is calculated as[38]

$$\chi = \beta + \frac{V_S}{RT}(\delta_S - \delta_P)^2 \tag{10}$$

where δ_S is the solubility parameter of the solvent; β, a lattice constant whose value was taken as 0.34;

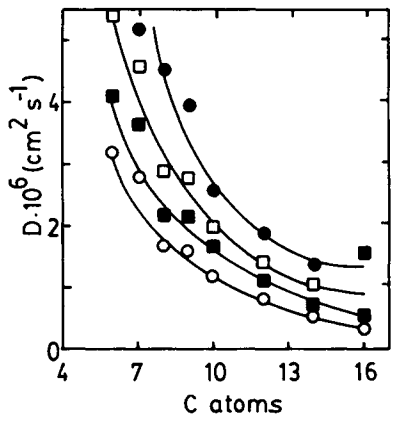

Figure 8 Dependence of diffusion coefficient on the number of carbon atoms of *n*-alkanes at temperatures given in Figure 4.

and RT, the usual energy term. To calculate χ by the above method, a prior knowledge of the solubility parameter, δ_P, of the polymer is necessary. For this purpose, the procedure suggested by Gee[39] and Takahashi[40] was used to compute δ_P of the polymer. Using this value for δ_P, the values of χ were calculated from eq. (10). The values of $\bar{M}_C$ were then calculated from eq. (8). These results are included in Table V. The values of $\bar{M}_C$ increase with increasing chain length of n-alkanes, suggesting a relationship between polymer chain entanglements with the solvent size. The values of $\bar{M}_C$ increase from about 92 for n-pentane to 521 for n-hexadecane. However, for 1,2,3,4-tetrahydronaphthalene, we did not obtain reliable datum and, hence, it is not reported. A comparison of $\bar{M}_C$ data with the OI values suggests that, in general, these values and the $\bar{M}_C$ data vary in accordance with the penetrant chain length in the same manner.

Diffusion in rubbery polymers also seems to bear direct relationships with some of the important properties such as viscosity,[41] η, dielectric constant, ε, refractive index, n_D, and speed of sound, u, in solvents. In the present systems, we found that η and ε show a systematic behavior with penetrant diffusivity (Fig. 9). Similarly, the molar refraction, $[R]$, of the liquid calculated from the Lorenz–Lorentz formula[42]

$$[R] = \frac{n_D^2 - 1}{n_D^2 + 2}\frac{M}{\rho} \tag{11}$$

(where M is molecular weight of the liquid, and ρ, its density) shows a decreasing trend with diffusion coefficients. The Rao's molar sound function, R, calculated as[43]

$$R = u^{1/3}V, \tag{12}$$

shows the same dependency (see Fig. 9). In eq. (12), V is molar volume of the solvent.

Concentration Dependence of Diffusion Coefficients

It may be noted that solvent diffusivity in rubbery polymers is dependent on the concentration. With an increase in sorption, the solvent concentration continues to build up at the membrane surface and, later, inside the core matrix and, thus, D becomes concentration-dependent. To investigate this effect, we analyzed the concentration dependence of diffusivity for those systems that exhibit an anomalous sorption diffusion behavior.[23]

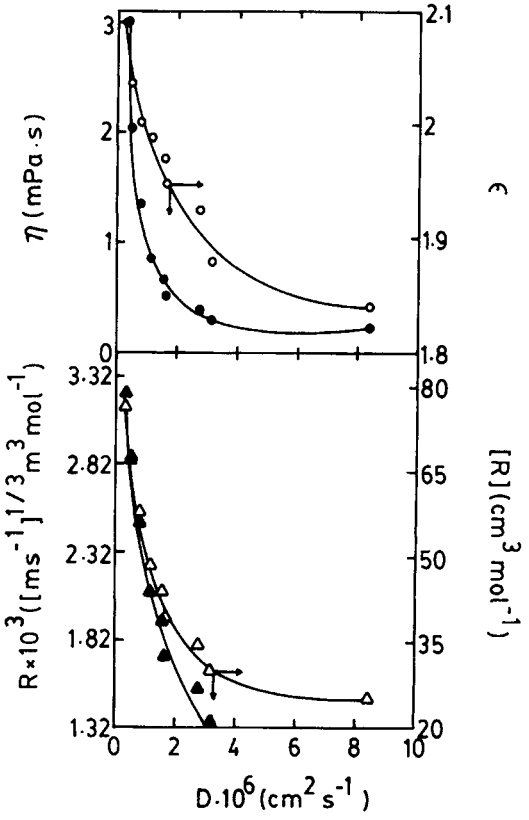

Figure 9 Relationship between (●) viscosity, (○) dielectric constant, (△) molar refractivity, and (▲) Rao's molar sound function with diffusivity for Santoprene + n-alkanes at 25°C.

The plots of D vs. wt % concentration for n-pentane to n-octane, n-nonane to n-hexadecane, and for 2,2,4-trimethylpentane, cyclohexane, and 1,2,3,4-tetrahydronaphthalene at 25°C are displayed in Figure 10. In all cases, an increase in D is observed up to about 70–75 wt % penetrant concentration. The heights of the maxima in these concentration intervals show a decrease from n-pentane to n-hexadecane. With cyclohexane and 2,2,4-trimethylpentane, the shapes of D vs. wt % concentration curves are somewhat identical. In the case of 1,2,3,4-tetrahydronaphthalene, the dependence is somewhat unsymmetric. These observations follow the swelling trends of the Santoprene membrane in the presence of n-alkanes. This observation is also consistent with the report of Waksman et al.[44] for rubbery systems and liquid organics.

Sorption Kinetics

Most cross-linked polymers exhibit swelling in the presence of aggressive solvent media. Such limited

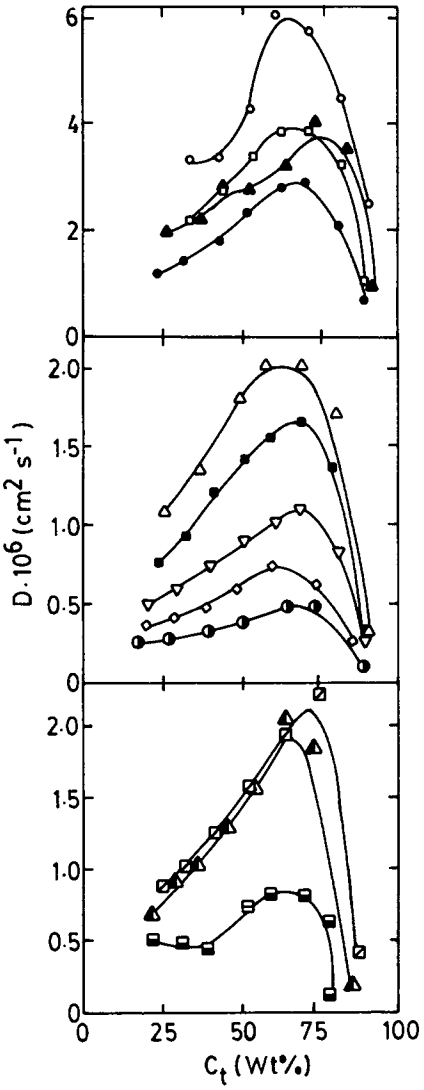

Figure 10 Concentration dependence of diffusion coefficient for Santoprene + alkanes at 25°C. Symbols are the same as in Figures 2 and 7.

swelling in semicrystalline polymers may be attributed to sorption kinetic phenomenon. In continuation of our earlier research,[45] the sorption in rubbery polymers can be used to calculate the first-order kinetic rate constant, k_1, by using

$$k_1 t = \ln[M_\infty/(M_\infty - M_t)] \tag{13}$$

A representative plot of $\log(M_\infty - M_t)$ vs. t is shown in Figure 11. For all solvents, the plots exhibit negative slopes with slight curvatures. The calculated k_1 values in the temperature interval 25–70°C are given in Table VIII. In all cases, the kinetic rate constants follow the regular trend of increase with temperature and decrease with increasing solvent size. This is expected because diffusivity is proportional to k_1 at long sorption times. Thus, the terms $n \geq 1$ and $\ln(8/\pi^2)$ can be ignored so that eq. (7) simplifies to give

$$\ln\left(\frac{M_\infty}{M_\infty - M_t}\right) \cong \frac{\pi^2 D t}{h^2} \tag{14}$$

Equation (14) is identical to eq. (13) when

$$k_1 = \frac{\pi^2 D}{h^2} \tag{15}$$

For extensive swelling, h^2 obviously does not remain constant and, hence, D increases due to the influx of the solvent into the polymer matrix material. As long as the increase in D matches h^2, the values of k_1 in eq. (15) remain nearly constant, so that eq. (13) or eq. (14) is obeyed approximately. Thus, the first-order kinetics seems to apply to the present systems.

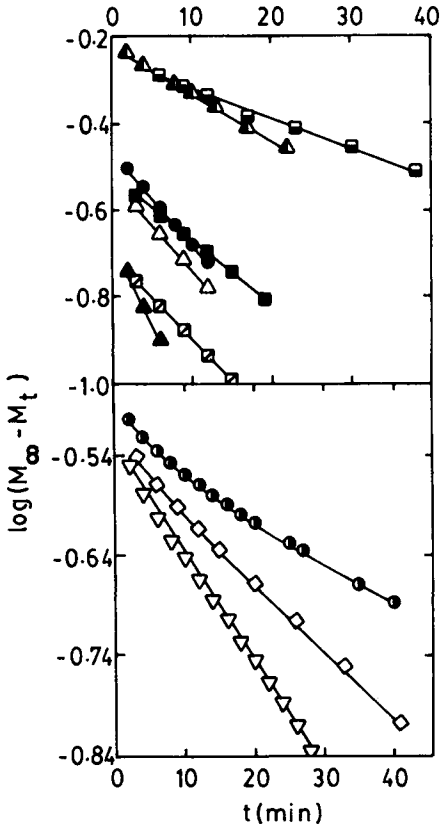

Figure 11 First-order kinetics plots for Santoprene + alkanes at 25°C. Symbols are the same as in Figures 2 and 7.

Table VIII First-order ($k_1 \times 10^2$, min^{-1}) and Second-order ($k_2 \times 10^2$, mol^{-1} min^{-1}) Rate Constants for Santoprene + Alkanes at Different Temperatures Obtained from Sorption and Resorption Experiments

	Temperature (°C)				
	25		40	55	70
Alkane	S	RS		S	
			k_1		
n-Pentane	2.56	3.10	[a]	[a]	[a]
n-Hexane	9.08	2.26	10.23	13.32	[a]
n-Heptane	8.15	1.94	12.30	12.72	18.87
n-Octane	5.05	1.46	6.42	8.04	13.39
n-Nonane	4.81	1.10	6.34	7.94	11.19
n-Decane	3.44	0.99	4.52	6.02	6.82
n-Dodecane	2.44	[b]	3.15	3.91	5.33
n-Tetradecane	1.57	[b]	2.00	3.08	3.85
n-Hexadecane	1.05	[b]	1.94	1.52	2.77
2,2,4-Trimethylpentane	4.44	0.93	5.32	6.88	8.37
Cyclohexane	2.51	1.03	3.69	4.83	5.38
1,2,3,4-Tetrahydronaphthalene	1.60	0.44	2.25	2.56	3.04
			k_2		
n-Pentane	170.14	26.51	[a]	[a]	[a]
n-Hexane	134.57	15.61	177.39	193.87	[a]
n-Heptane	102.70	10.43	153.27	151.93	260.28
n-Octane	46.92	7.50	60.36	74.59	178.14
n-Nonane	54.08	6.01	69.28	83.52	124.28
n-Decane	38.02	4.82	46.15	58.64	64.57
n-Dodecane	27.57	[b]	33.29	38.41	54.93
n-Tetradecane	16.80	[b]	21.27	32.12	37.06
n-Hexadecane	9.41	[b]	15.42	18.58	27.13
2,2,4-Trimethylpentane	75.40	5.02	83.56	10.19	11.74
Cyclohexane	12.45	3.57	19.92	23.82	22.53
1,2,3,4-Tetrahydronaphthalene	8.86	1.57	12.15	12.03	12.81

[a] Data not obtained due to their low boiling points.
[b] Data not obtained due to their high boiling points.

When swelling becomes considerable and the increase in h^2 exceeds the increase in D to a point where the variation in k_1 and the deviation from the first-order kinetics becomes significant, the second-order kinetics may be used from the following considerations[46-48]:

$$\frac{t}{Q} = A + Bt \tag{16}$$

where A and B are numerical constants. At long times, $Bt > A$, so that $B = 1/M_\infty$. At short times, $A > Bt$, so that the quantity $1/A = t \xrightarrow{lim} 0 (dC/dt)$ represents the initial rate of swelling, when the polymer network begins to relax in response to the osmotic pressure. The equation for second-order swelling is then given as

$$\frac{dC}{dt} = k_2(M_\infty - M_t)^2 \tag{17}$$

where k_2 is the second-order rate constant. The integrated form of the equation representing the swelling rate at time t is given by

$$M_t = \frac{k_2 M_\infty^2 t}{1 + k_2 M_\infty t} \tag{18}$$

which upon further simplification gives

$$k_2 t = \frac{M_t}{M_\infty (M_\infty - M_t)} \quad \text{or}$$

$$k_2 t = \frac{1}{M_\infty - M_t} - \frac{1}{M_\infty} \tag{19}$$

where $k_2 = 1/M_\infty^2$. The dimensions of k_2 are mol^{-1} min^{-1} (see Table VIII). Detailed explanations for the use of the second-order swelling kinetics has been given by Schott.[46]

A typical second-order kinetic plot for n-alkanes (except n-pentane and n-heptane) at 25°C given in Figure 12 supports the use of the second-order kinetics for systems of this study. The second-order kinetic plot follows the curvature behavior over the entire swelling process. However, to estimate the second-order kinetic rate constant values, we need to consider only the initial portion of the swelling curve. The early portion of this curve is a straight line. From the slope of this line, the values of k_2 have been obtained; these values are generally smaller than the k_1 values for all the systems.

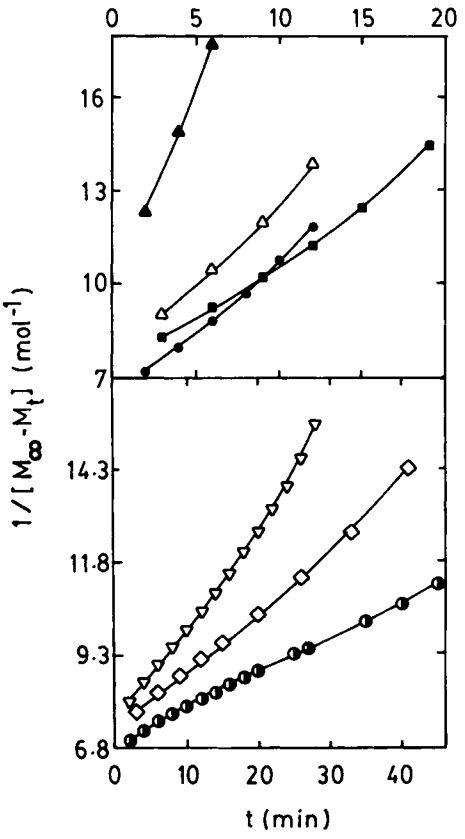

Figure 12 Second-order kinetics plots for Santoprene + alkanes at 25°C. Symbols are the same as in Figures 2 and 7.

Temperature Effects and Activation Parameters

Significant advances have been made over the past decades to develop a microscopic description of the diffusion phenomenon in polymers and that diffusion in rubbery polymers is very different than in glassy polymers.[49] According to molecular models of rubbery polymers above the glass transition temperatures, the Arrhenius relation is valid experimentally, but curved plots are also observed when higher temperatures are used.[50] In the present experimental systems, the following Arrhenius relation is obeyed for diffusion

$$D = D_0 \exp(-E_D/RT) \tag{20}$$

where E_D is the activation energy of diffusion, which is a function of the intra- and interchain forces that must be overcome in order to create the space for a unit diffusional jump of the penetrant molecule, D_0 is a preexponential factor, and RT has the conventional usual meaning. The activation energy will be greater the larger the penetrant molecule, the stronger the polymer cohesive energy, and the more rigid the polymer-chain segments.

In an analogous manner, the sorption coefficient, S, can be expressed using van't Hoff equation with a preexponential factor S_0 as

$$S = S_0 \exp(-\Delta H_S/RT) \tag{21}$$

where ΔH_S is the heat of sorption and is a composite parameter involving the contributions from (i) Henry's law needed for the formation of a site and the dissolution of the species into that site—the formation of a site involves an endothermic contribution, and (ii) Langmuir's (hole-filling)-type sorption mechanisms, in which case the site already exists in the polymer matrix and sorption by hole filling gives exothermic heats of sorption.

Because the transport phenomenon involves both the sorption and diffusion processes, the permeability coefficient, $P(\equiv D \cdot S)$, may also be expressed in a similar manner and the activation energy, E_P, for the permeation process is given as

$$E_P = E_D + \Delta H_S \tag{22}$$

Since in the present polymer–solvent systems the values of S, P, and D showed an increase with a rise

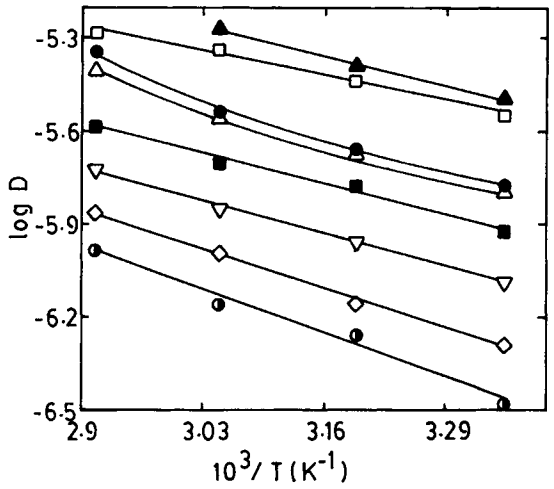

Figure 13 Arrhenius plots for the dependence of log D vs. $1/T$ for Santoprene + alkanes. Symbols are the same as in Figures 2 and 7.

in temperature, eqs. (20) and (21) are used to calculate E_D and ΔH_S values from the least-squares procedure. Figure 13 displays the plot of log D vs. $1/T$, wherein the dependence follows linearity in the investigated temperature interval. Using eq. (22), the E_P values have been calculated. These results are summarized in Table IX. Activation parameter values do not show any regular trend with penetrant size. The values of E_D and E_P vary from a minimum of 12 kJ/mol for *n*-heptane to a highest value of 21 kJ/mol for *n*-hexadecane. The E_D or E_P values for 2,2,4-trimethylpentane are lower than those for *n*-octane; similarly, the E_D and E_P values for 1,2,3,4-tetrahydronaphthalene are lower than those for cyclohexane. However, there is an increase of about 6 kJ/mol in the E_D value of 2,2,4-trimethylpentane when compared to *n*-octane.

For all penetrants except *n*-heptane and *n*-octane, ΔH_S values are positive, suggesting the sorption to be dominated by Henry's mode with an endothermic contribution. However, *n*-octane exhibits a more negative ΔH_S value than does *n*-heptane, suggesting Langmuir-type sorption with these penetrants. An interesting question is whether the solvent molecules penetrate into pores (or voids) that already exist in the polymer before solvent sorption or whether they create new pores. To answer this question, the volumes of the Santoprene saturated with the solvents were measured and compared to the dry volume of Santoprene. If solvents simply fill the free volume, then polymer volume should increase. In almost all cases, the volume of Santoprene is increased due to solvent influx due possibly to a contribution from the Henry's sorption mode. However, the volume increases are not greatly significant, i.e., the ratio $(\Delta V)/V$ varies from 0.26 for *n*-pentane to about 0.69 for cyclohexane at 25°C.

CONCLUSIONS

In polymer applications involving solvent exposure, an understanding about the sorption and transport of solvents through the polymer is important in a variety of areas such as pervaporation, barrier packaging, controlled delivery of biologically active materials, and plasticizer migration. These varied applications reveal that the study of polymer–solvent interactions is very crucial for their successful applications. The transport parameters in this study were found to decrease linearly with an increase in the size of *n*-alkanes. The diffusivity values of 2,2,4-trimethylpentane at all temperatures are lower and E_D is higher than the corresponding values for *n*-octane. This is attributed to the rigidity of the 2,2,4-trimethylpentane molecule. The change in the size of alkanes showed an increasing resistance to diffusion. At higher temperatures, the increase in diffusion and relaxation rates of Santoprene, accompanied by an increase in the polymer free volume, might have resulted in a higher equilibrium penetrant uptake.

The observed overshoot effect is attributed to the leaching-out phenomenon. Transport kinetics has been studied in terms of the first-order and second-order kinetic model. However, it is difficult to characterize the overall transport kinetics with a specific experimental parameter and to decide between the

Table IX Activation Parameters (E_D, E_P, and ΔH_S all in kJ/mol) for Santoprene + Alkanes

Alkane	E_D	E_P	ΔH_S
n-Hexane	14.28	16.34	2.06
n-Heptane	11.88	12.12	−0.24
n-Octane	18.39	16.76	−1.63
n-Nonane	16.82	18.96	2.14
n-Decane	14.12	17.29	3.18
n-Dodecane	15.52	18.64	3.11
n-Tetradecane	18.75	21.23	2.48
n-Hexadecane	21.07	21.83	0.76
2,2,4-Trimethylpentane	12.00	14.08	2.08
Cyclohexane	15.06	19.28	4.21
1,2,3,4-Tetrahydronaphthalene	12.58	17.75	5.17

use of the first-order or second-order sorption kinetics in the present systems. To the best of our knowledge, the first-order kinetic rate constant results may be more appropriate in the present work due to the limited swelling of Santoprene sheets in the presence of the chosen solvent media. It was shown that the changes in the transport kinetics during S–RS experiments are caused by the changes in the relative rates between the polymer chain relaxation and the penetrant diffusion during sorption. The concentration dependence of diffusion coefficients has been studied.

We are thankful to the Council of Scientific and Industrial Research [Grant No. 01(1239)/92/EMR-II] for a major financial support of this study. We also thank Mr. Brant Fletcher of Advanced Elastomer Systems, St. Louis, MO, for a free supply of Santoprene samples used in this study.

REFERENCES

1. P. V. Kulkarni, S. B. Rajur, P. Antich, T. M. Aminabhavi, and M. I. Aralaguppi, *J. Macromol. Sci. Rev. Macromol. Chem. Phys.*, **C30,** 441 (1990).
2. N. A. Peppas and R. W. Korsmeyer, in *Hydrogels in Medicine and Pharmacy,* N. A. Peppas, Ed., CRC Press, Boca Raton, FL, 1987, Vol. III.
3. H. Coll and C. G. Searles, *Polymer,* **29,** 1266 (1988).
4. R. B. Seymour, *Engineering Polymer Source Book,* McGraw-Hill, New York, 1990.
5. J. Landois-Garza and J. H. Hotchkiss, *Food and Packaging Interactions,* ACS Symposium Series 365, American Chemical Society, Washington, DC, 1987, p. 53.
6. G. Strandburg, P. T. DeLassus, and B. A. Howell, in ACS Symposium Series 423, W. J. Koros, Ed., American Chemical Society, Washington, DC, 1990, p. 333.
7. T. M. Aminabhavi, R. S. Khinnavar, S. B. Harogoppad, U. S. Aithal, Q. T. Nguyen, and K. C. Hansen, *J. Macromol. Sci. Rev. Macromol. Chem. Phys.*, **34,** 139 (1994).
8. M. O. David, Q. T. Nguyen, and J. Neel, *J. Membr. Sci.*, **73,** 129 (1992).
9. R. Y. M. Huang, Ed., *Pervaporation Membrane Separation Processes,* Elsevier, New York, 1991.
10. J. Crank, *Mathematics of Diffusion,* 2nd ed., Clarendon, Oxford, 1975.
11. N. A. Peppas and K. G. Urdahl, *Polym. Bull.*, **33,** 2669 (1986).
12. K. G. Urdahl and N. A. Peppas, *J. Appl. Polym. Sci.*, **33,** 2669 (1987).
13. K. G. Urdahl, and N. A. Peppas, *Polym. Eng. Sci.*, **28,** 96 (1988).
14. N. M. Franson and N. A. Peppas, *J. Appl. Polym. Sci.*, **28,** 1299 (1983).
15. C. M. Walker and N. A. Peppas, *J. Appl. Polym. Sci.*, **39,** 2043 (1990).
16. D. Kim, J. M. Caruthers, and N. A. Peppas, *Macromolecules,* **26,** 1841 (1993).
17. L. Y. Shieh and N. A. Peppas, *J. Appl. Polym. Sci.*, **42,** 1579 (1991).
18. G. W. R. Davidson and N. A. Peppas, *J. Control Rel.*, **3,** 243 (1986).
19. G. W. R. Davidson and N. A. Peppas, *J. Control Rel.*, **3,** 259 (1986).
20. M. J. Smith and N. A. Peppas, *Polymer,* **26,** 569 (1985).
21. R. W. Korsmeyer and N. A. Peppas, *J. Control Rel.*, **1,** 89 (1984).
22. H. E. Johnson, S. J. Clarson, and S. Granick, *Polymer,* **34,** 1960 (1993).
23. S. B. Harogoppad and T. M. Aminabhavi, *Macromolecules,* **24,** 2598 (1991).
24. R. S. Khinnavar and T. M. Aminabhavi, *J. Appl. Polym. Sci.*, **42,** 2321 (1991).
25. T. M. Aminabhavi and H. T. S. Phayde, *Polymer,* in press.
26. J. A. Riddick, W. B. Bunger, and T. K. Sakano, *Techniques in Chemistry,* Vol. II, *Organic Solvents,* 4th ed., Wiley, New York, 1986.
27. T. M. Aminabhavi, R. S. Munnolli, W. M. Stahl, and S. V. Gangal, *J. Appl. Polym. Sci.*, **48,** 857 (1993).
28. R. S. Khinnavar and T. M. Aminabhavi, *Polymer,* **34,** 1006 (1993).
29. S. B. Harogoppad and T. M. Aminabhavi, *J. Appl. Polym. Sci.*, **46,** 725 (1992).
30. S. B. Harogoppad and T. M. Aminabhavi, *Polymer,* **32,** 870 (1991).
31. J. D. Ferry, in *Viscoelastic Properties of Polymers,* Wiley, New York, 1970.
32. M. Salem, A. F. A. Asfour, D. DeKee, and B. Harrison, *J. Appl. Polym. Sci.*, **37,** 617 (1989).
33. W. R. Brown and G. S. Park, *J. Paint Technol.*, **42,** 16 (1970).
34. W. R. Brown, R. B. Jenkins, and G. S. Park, *J. Polym. Sci. Polym. Symp.*, **41,** 45 (1973).
35. A. Aitken and R. M. Barrer, *Trans. Faraday Soc.*, **51,** 116 (1955).
36. P. J. Flory, *Principles of Polymer Chemistry,* Cornell University Press, Ithaca, NY, 1953.
37. P. J. Flory and J. Rehner, Jr., *J. Chem. Phys.*, **11,** 521 (1943).
38. G. M. Bristow and W. F. Watson, *Trans. Faraday Soc.*, **54,** 1731 (1958).
39. G. Gee, *Trans. Faraday Soc.*, **38,** 418 (1942); **40,** 468 (1944).
40. S. Takahashi, *J. Appl. Polym. Sci.*, **28,** 2847 (1993).
41. N. Vahdat, *J. Appl. Polym. Sci.*, **42,** 3165 (1991).
42. C. J. F. Bottcher, *Theory of Electric Polarization,* Elsevier, Amsterdam, 1952.

43. M. R. Rao, *Curr. Sci.*, **8,** 510 (1939); *Chem. Phys.*, **9,** 682 (1941).
44. L. S. Waksman, N. S. Schneider, and N. H. Sung, in *Barrier Polymers and Barrier Structures,* W. J. Koros, Ed., American Chemical Society, Washington, DC, 1990, Chap 20.
45. T. M. Aminabhavi and S. B. Harogoppad, *J. Chem. Ed.*, **68,** 343 (1991).
46. H. Schott, *J. Macromol. Sci. Phys.*, **B31,** 1 (1992).
47. C. M. Ofner and H. Schott, *J. Pharm. Sci.*, **75,** 790 (1986).
48. C. M. Ofner and H. Schott, *J. Pharm. Sci.*, **76,** 715 (1987).
49. T. M. Aminabhavi, U. S. Aithal, and S. S. Shukla, *J. Macromol. Sci. Chem. Phys.*, **C28**(34), 421 (1988).
50. M. J. Hayer and G. S. Park, *Trans. Faraday Soc.*, **51,** 1134 (1955).

Received April 14, 1994
Accepted September 7, 1994